Sensing and Bio-Sensing Research 45 (2024) 100682

Contents lists available at ScienceDirect

Sensing and Bio-Sensing Research

journal homepage: www.elsevier.com/locate/sbsr

Design of hexagonal shaped spectroscopy based biosensor for the detection of tuberculosis

Rakib Hossen [a], Md. Selim Hossain [b], Sadia Afrin Mim [c], Md. Al-Amin [d], Sabbir Ahmed [e], Md. Ashrafuzzaman [f], Md. Ashiq Salahin [f], Shuvo Sen [g,*]

[a] Department of Cyber Security Engineering, Bangabandhu Sheikh Mujibur Rahman Digital University, Bangladesh, Kaliakoir, Gazipur 1750, Bangladesh
[b] Department of Electronics and Communication Engineering (ECE), Hajee Mohammad Danesh Science and Technology University (HSTU), Dinajpur 5200, Bangladesh
[c] Department of Pathology, Faculty of Veterinary Science, Bangladesh Agricultural University, Mymensingh, Bangladesh
[d] Department of Electrical and Electronic Engineering (EEE), Daffodil International University (DIU), Dhaka, Bangladesh
[e] Department of Educational Technology and Engineering, Bangabandhu Sheikh Mujibur Rahman Digital University, Bangladesh, Kaliakoir, Gazipur 1750, Bangladesh
[f] Department of Pharmacology, Faculty of Veterinary Science, Bangladesh Agricultural University, Mymensingh, Bangladesh
[g] Department of Information and Communication Technology (ICT), Mawlana Bhashani Science and Technology University (MBSTU), Santosh, Tangail 1902, Bangladesh

ARTICLE INFO

Keywords:
Biosensor
Tuberculosis
Hexagonal model
Spectroscopy
Optical sensor

ABSTRACT

A proposal has been made to identify tuberculosis cells using a novel compact sensor based on photonic crystal fiber: PCF in accordance with hexagonal spectroscopy. This proposed structure, which consists of a closely packed hexagonal air hole in the cladding region and a hollow-core area, possesses a very low loss of 6.30×10^{-8} dB/m and an exceptionally high sensitivity of up to 91.75 % (tuberculosis cell for 1.345). Numerous optical parameters have been identified and assessed, comprised of the numerical aperture, the V-parameter, or normalized frequency (V_{eff}), and the effective area (A_{eff}). The operational wavelength range is defined as 0.80–3.0 THz. The numerical investigation of the properties of the proposed TB sensors is performed within the environment of COMSOL Multiphysics (Version 5.3) using FV-FEM stands for the full vector finite element method. PCF sensors composed of hexagonal lattice in a circular form with ZEONEX as the backdrop material is intended to boost the sensitivity response in comparison to the earlier works. Additionally, the sensor that is being displayed achieves a single modality throughout its whole operational wavelength range. This proposed sensor may play a significant role in identifying tuberculosis thanks to its superior sensitivity response and extremely minimal confinement loss. So, it is clearly seen that this sensor could be used to bio-medical sectors with process of terahertz (THz) wave pulse.

1. Introduction

Photonic crystal fiber (PCF) sensors have demonstrated significant potential in sensing applications, due to their adaptable design. Minimal confinement reduction [1], strong birefringence [2], and profound nonlinearity [3] are just a few benefits that PCF possesses over traditional fiber. There are numerous uses for PCF in the field of sensing thanks to its added benefits of reduced computing time, low cost, and good outcomes. PCF sensors have been used to measure temperature [4], hydrostatic pressure [5], salinity [6], gas [7], the refractive index of blood components [8], and to find dangerous food additives [9,10]. *Mycobacterium tuberculosis* is a common and possibly fatal illness that causes tuberculosis. Nearly one-third of the world's population is thought to be tuberculosis (TB) infected. The TB bacteria can stay dormant in the body for a very long time without doing any harm, but as a person loses strength when the tuberculosis microbes activate, they might commence impacting beyond the pulmonary system, and additional anatomical regions. An estimated 1.5 million people every year pass away from TB. When a person with tuberculosis coughs or sneezes, it can spread via the air [11]. Other diseases like HIV, which impairs immunity, can make tuberculosis worse. The majority of tuberculosis cases occur in underdeveloped nations with inadequate resources for detecting and treating the illness [12].

The WHO wants to eradicate tuberculosis on a global scale. According to this plan, the number of deaths must be reduced by 75 % by 2025 (relative to 2015) and by 95 % by 2035 [13]. Traditional TB

* Corresponding author.
E-mail address: shuvombstu.it12009@gmail.com (S. Sen).

https://doi.org/10.1016/j.sbsr.2024.100682
Received 22 January 2024; Received in revised form 15 August 2024; Accepted 29 August 2024
Available online 30 August 2024

detection and diagnosis techniques can be expensive and time-consuming. These techniques include bacterioscopy, mantoux testing, swab culture, and chest radiology [14]. For the identification of mycobacteria by polymer chain reaction (PCA), a method referred to as specific DNA sequence amplification is employed [15]. Due to the need for skilled personnel and pricey testing equipment, this procedure is costly and time-consuming, and it may produce inaccurate results [16]. In developing nations, several tuberculosis testing techniques are not always accessible. An efficient method that has a high sensitivity, a quick detection time, cost effectiveness, and ease of use is needed to solve these issues. The design flexibility of PCF makes it potentially useful for tuberculosis detection. Scientists have been working on optical biosensors for the past ten years to quickly and affordably detect the bacterial cells that cause a variety of diseases. Due to their sensing properties, ease of handling, straightforward design, and small size, photonic crystal fiber can be based on wherein surface plasmon resonance (SPR) among the numerous methods utilized [17] and spectroscopy [18]. Due to their exceptional performance, PCF-based fibers are receiving interest in the field of disease detection. Hsu et al. (2014) used telecommunication wavelengths to detect the deoxyribonucleic acid (DNA) of *Mycobacterium tuberculosis* (MTB) in order to demonstrate SPR-based PCF. The wavelengths can be increased to increase sensitivity. The design is complicated, yet [19]. Trzaskowski et al. created a portable SPR device in 2017. 10 mg/ml quantities of the secretory protein Ag85 from Mycobacterium TB can be detected [14]. By using the Transfer Matrix Method (TMM) to analyze the waveguide, in 2020, Ramanujam et al. introduced a ring mirror-defect-based PCF based on SPR for tuberculosis cell identification. This approach, however, also has considerable complexity [11]. Based on absorption spectroscopy, various designs have been examined.

This is the first time that a distinctive hexagonal structure for tuberculosis cell detection has been offered to the spectroscopic-based PCF sensor. The inquiry being proposed is entirely simulation-based. Software called Comsol Multiphysics has been used to conduct all of the observations. FV-FEM approach has also been applied to numerical analysis. Additionally, many optical characteristics are adjusted to improve response, producing a high sensitivity with minimal confinement loss. The sensor displays better results as a single modality. In comparison to recently published works [29–38], the sensitivity has been enhanced to readily detect tuberculosis cells. The maximum sensitivities are 91.75 %, 89.41 %, 91.74 %, 91.73 %, and 87.65 % and low confinement loss of are 6.30×10^{-8} dB/m, 6.50×10^{-8} dB/m, 6.25×10^{-8} dB/m, 6.35×10^{-8} dB/m, 6.45×10^{-8} dB/m for RI of1.345, 1.346, 1.347, 1.348 and 1.349 respectively as well as the structure's EML is reduced to 0.0211 cm^{-1} at an operating wavelength of 1Thz. Subsequently, examining the optical characteristics of the suggested sensor architecture clearly shows and reveals substantial values for relative sensitivity and negligible quantities between effective material loss and loss from confinement. Our findings highlight the suitability of the suggested PCF sensor design for real-world uses like as bio-sensing and bio-medical engineering in the detection of tuberculosis cells.

1.1. Design methodology and mode field distributions

Designing an incredibly sensitive sensor and little confinement loss is the key goal. In order to attain high sensitivity, the hexagonal structure in the cladding region was chosen, allowing for increased light-matter interaction with very little confinement loss. For the purpose of detecting TB cells, a new hexagonal structure design is put forth in this article. A geometric framework supports the H-PCF that, as shown in Fig. 1, consists of five strata of air apertures (AH) arranged in a hexagonal pattern. Diameters d_1 and A_1 of the cladding zone represent the distance across and pitch as specified by the proper design approach. The area of the cylindrical core's diameter is assumed to be d = 80 μm. In contrast, ZEONEX functions as a foundational fabric that facilitates the attainment of the intended enhanced RS and reduced CL. The

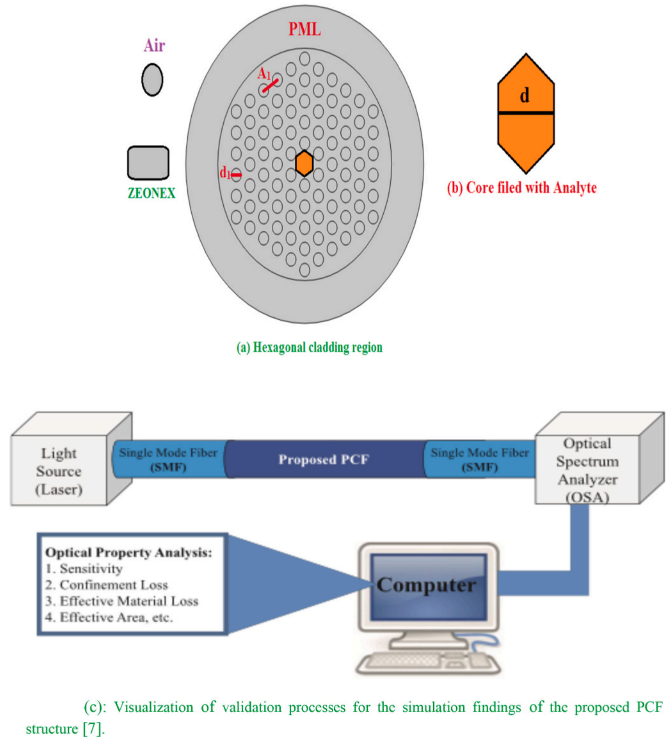

Fig. 1. Aesthetic representations of the terahertz-based PCF sensor under consideration: (a) Cladding region and (b) Hollow-core region.

rationale behind the selection of Zeonex as background material is that this particular borosilicate glass which has minimal optical loss, good thermal steadiness and suitability for a broad variety of wavelengths is employed in PCF for a various of photonic applications. The "air filling ratio," or d_1/A_1, enables streamlined production in the "cladding zone" of an expanding system. The H-PCF fiber is customized to operate within the terahertz recurrence wave-band of 0.80–3.0 THz through the utilization of a COMSOL Multiphysics software instrument based on PML and FEM. In the case of two layers, the optimal parameters are implementing a boundary condition of PML (Perfectly-matched layer (PML_1) =2150 μm and Perfectly-matched layer (PML_2) =2365 μm) with a 10 % thickness relative to the maximum fiber width: With a cladding pitch of $A_1 = A_2 = A_3 = A_4 = A_5 = 360$ μm and a cladding distance of $d_1 = 290$ μm, respectively. **(See details** Table 1**).**

In Fig. 1(c), light laser is transmitted in the proposed structure of PCF core and the optical spectrum analyzer (OSA**)** will shows data in the computer monitor to determine the guiding properties such as high sensitivity, low loss, effective mode index and effective area in the injected tuberculosis cell. Then, we find experimental data graphically

Table 1
The H-PCF structure's values and parameters.

Parameters	Values	Parameters	Values
Cladding pitch (A_1)	360 μm	Sensitivity tuberculosis cell (for 1.345)	91.75 %
Cladding distance (d_1)	290 μm	Effective area tuberculosis cell (for 1.345)	1.38×10^{-7} m^2
hollow core area (d)	80 μm	Confinement loss tuberculosis cell (for 1.345)	6.30×10^{-8} dB/m
Perfectly-matched layer (PML_1)	2150 μm	Effective material loss (EML)	0.0211 cm^{-1}
Perfectly-matched layer (PML_2)	2365 μm	–	–
–	–	–	–

usingMATLAB.

Fig. 1(c): Visualization of validation processes for the simulation findings of the proposed PCF structure [7].

In both polarization phases, as illustrated in Fig. 2, all light passes through the center of the core. (See Fig. 3.)

1.2. Experimental sensor system

Here, we have also presented the block diagram to detection tuberculosis cell with carefully by the following steps: Prepare a sample in the core area of H-PCF structure and place it in the experimental sensor system practically. The light source works as an interaction with the sample via the proposed H-PCF. Then, we achieve different types of refractive index (RI) based tuberculosis cell by the real-time data collection and data analysis procedure.

1.3. Guiding properties of tuberculosis sensor

The tuberculosis sensor's proposed spectroscopy-based structure for quick detection of various tuberculosis cell types with fixed refractive index (RI) values is depicted in Fig. 4. In the operating wavelength, the differences in the RI of the chosen tuberculosis cells are quite small, the RI of the background material, ZEONEX, was estimated [20].

The interaction of light with directed material is shown by the coefficient of relative sensitivity. The proposed hexagonal PCF's sensing response can be calculated by calculating relative sensitivity [21]:

$$R = \frac{n_r}{n_{eff}} \times E \tag{1}$$

The sample's index of refraction is n_r, which for tuberculosis cells ranges from 1.345 to 1.349; n_{eff}, the effective refractive index of guided modes at that specific terahertz wavelength; R, the relative sensitivity; and E, the amount of light interacting with the analytic.

Additionally, the entire light-matter interaction is computed as [22,23],

$$E = \frac{\int_{sample} R_e\left(E_x H_y - E_x H_y\right) dxdy}{\int_{total} R_e\left(E_x H_y - E_x H_y\right) dxdy} \times 100\% \tag{2}$$

The guiding modes' electric field components, represented by Ex, Ey, and magnetic field components, represented by Hx, Hy, respectively,

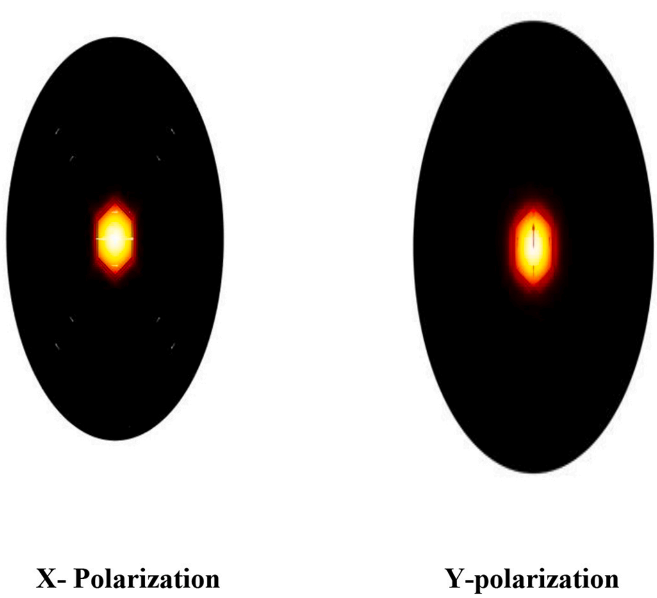

Fig. 2. Model mode field distribution for both polarizations within the operational frequency range of 1 THz.

ascertain the recommended sensor's relative sensitivity.

The sensitivity graph is shown for wavelengths between 0.8 THz and 3THz for TB cells with refractive indices between 1.345 and 1.349. It is clear that the sensitivity rises with increasing wavelength up to 1.5 THz before progressively starting to fall. The core power fraction achieves its maximum value at 0.8 THz wavelength due to the strongest light interaction, which is the cause of this. The relative sensitivity decreases as the value of n_{eff} rises continuously. Therefore, 1 THz is selected as the operating wavelength. Fig. 4 demonstrates that the refractive index from 1.345 to 1.349 at the ideal wavelength of 1THz has the maximum sensitivity. The maximum sensitivities are 91.75 %, 89.41 %, 91.74 %, 91.73 %, and 87.65 %, for RI of 1.345, 1.346, 1.347, 1.348 and 1.349 respectively. The variances are slight and the sensitivity value for all refractive indexes is greater than 92 %. The sensor is more effective if its relative sensitivity performance is at its highest level. When compared to earlier research, these sensitivity values are extremely high.

The modes of optical fiber are controlled by the normalized frequency or V-parameter. Single-mode and multi-mode guiding modes are the two distinct classifications. Applying expression (4) evaluates the V-parameter. Fig. 5 depicts the relationship between a V parameter and wavelength. The reported single-mode characteristics of the given hexagonal are observed in the 0.8 THz and 3THz wavelength range. The estimated value is less than 2.405, as can be seen, and the V values are extremely close to one another. For the purpose of highlighting the discrepancies, the zoom area has been added to the above figure. As a result, it only displays one modality. As a result, the proposed hexagonal PCF can be used for sensory long-range, which is a strong suit of PCF-based sensors. The graph clearly shows that the value of the V-parameter increases as the wavelength increases. (See Fig. 6.)

The subsequent equation is employed to ascertain the V-parameters of the H-PCF [24]:

$$V = \frac{2\pi r f}{c} \sqrt{n^2{}_{co} - n^2{}_{cl}} \leq 2.045 \tag{4}$$

Where, in which n_{co} denotes the core area's refractive index which is obtained from the software COMSOL Multiphysics between 0.08 and 3 THz (THz) in frequency and where ncl = 1 represents the cladding area's refractive index that is V = 2.93216*SQRT (n_{co} * n_{co} - n_{co} * n_{co}) and r denotes the radius of the fiber core.

Regarding the increase in frequency within the THz range, the V-parameter fluctuates with the intention of H-PCF as depicted in Fig. 5, singular mode fiber, under optimal design conditions. Based on the graph, an analysis is conducted that from approximately 2.10 THz onwards, the V-parameter increases proportionally with the frequency in the terahertz segment. Once the frequency reaches approximately 3 THz, the V-parameter continues to increase at a slightly slower rate compared to its initial value of 2.10 THz.

Confinement loss (CL) develops as a result of their permeable characteristics. Transmitting electricity from principally responsible for confinement loss is the cladding's core. In order to perform the calculation of CL, it is considered the imaginary component of the index of effective refraction. The loss confinement is computed using the following expression [25].

$$L_c\left[\frac{dB}{m}\right] = 8.686 K_0\, Im\left[n_{eff}\right] \tag{5}$$

$$K_0 = 2\pi\left(\frac{f}{c}\right) \tag{6}$$

The electromagnetic waves' frequency (f) and speed ($c = 3 \times 10^8$ ms^{-1}) are given in this expression. In addition, I_m is the imaginary component and K_0 is the number of free waves.

The hexagons, therefore, are tightly packed together in the cladding area; there is very little confinement loss. At an operating wavelength of 1 THz, the confinement losses are 6.30×10^{-8} dB/m, 6.50×10^{-8} dB/m, 6.25×10^{-8} dB/m, and 6.35 × 10–8 dB/m, 6.45 × 10–8 dB/m for 1.345,

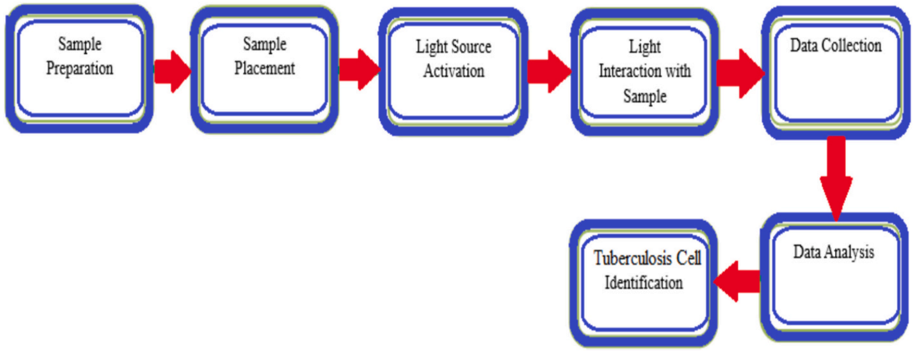

Fig. 3. Representation of block diagram for experimental system and identification of tuberculosis cell via the H-PCF structure [8].

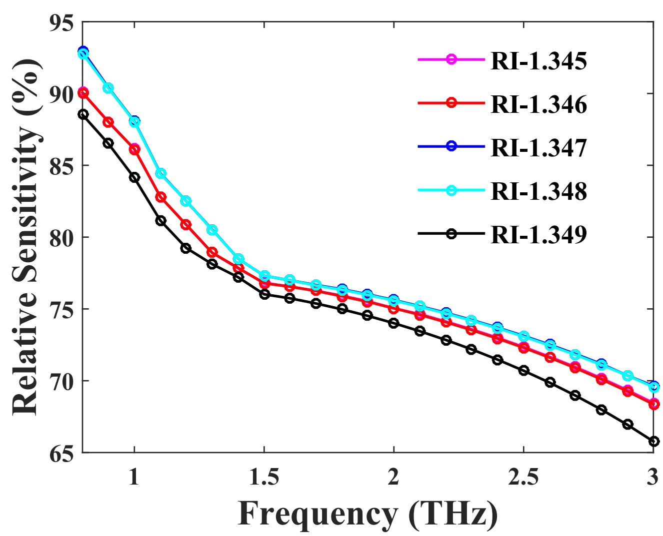

Fig. 4. RS is plotted against frequency for tuberculosis cells ranges from 1.345 to 1.349.

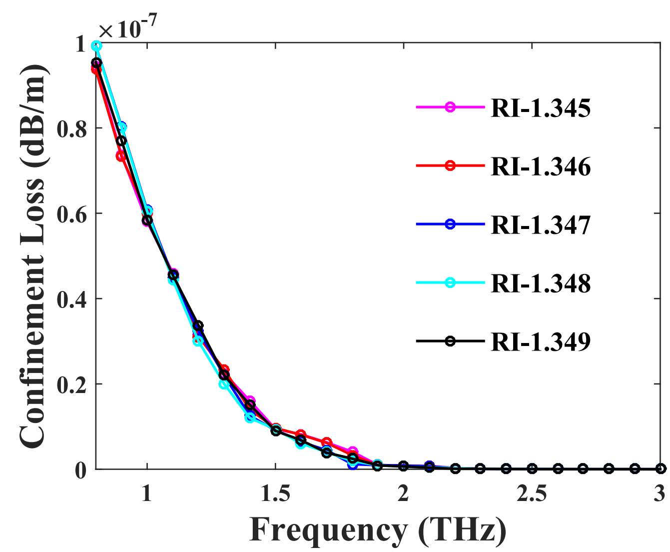

Fig. 6. At optimal parameters, the behavior of CL in the THz region with respect to frequency.

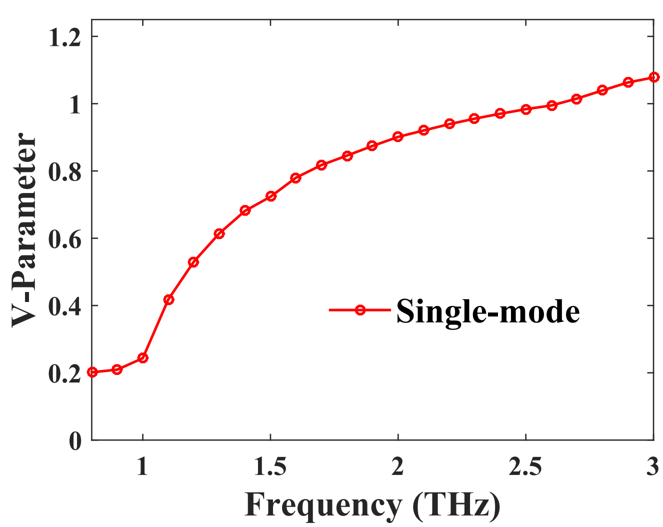

Fig. 5. Features of V-parameter for optimal parameters vs frequency at THz.

1.346, 1.347, 1.348, and 1.349 respectively.

The region of the effective mode is A_{eff}. A lower effective area is better for the nonlinearity effect, but communication devices can use a higher value. Eq. (7) provides the empirical formula for the effective area [26].

$$\text{Aeff} = \frac{\left[\int I(rt)rtdrt\right]^2}{\left[\int I^2(rt)drt\right]^2}, (\text{m}^2) \tag{7}$$

The effective mode area of the newly introduced TB sensor is explored. Here, $[\int I(rt)rtdrt]^2$ indicates the Integration of core power and $[\int I^2(rt)drt]^2$ is the total power. It is simple to determine the effective area from the power spectrum measurements. A_{eff} is a crucial factor in the optical signal's propagation. Eq. (7) provides the absolute-Area through which the electromagnetic signal travels.

The effective area grows with wavelength at working wavelengths between 0.8 THz and 3THz, as depicted in Fig. 7. The effective region subsequent to the ideal PCF fiber configuration is illustrated in Fig. 7. Within the range of 0.8 to 3 THz, the EA decreases. Along the THz waveguide, the low CL and high RS are denoted by the substantial EA. The EA are 1.38×10^{-7}, 1.40×10^{-7} m^2 and 1.41×10^{-7} m^2, 1.42×10^{-7} and 1.45×10^{-7} m^2 at 1 THz for RI of 1.345, 1.346, 1.347, 1.348 and 1.349 respectively.

The numerical aperture must be greater for applications involving large-scale sensing. A study is done on the TB sensor's NA. Determine the numerical aperture utilizing the subsequent Eq. [27]:

$$\text{NA}(\text{R}, \alpha) = \sqrt{n_{core}^2 - n_{cladding}^2 \left(\frac{R + r}{\text{R} + \alpha}\right)^2} \tag{8}$$

Where, n_{core} and n_{cladding} are the fiber core's and the cladding's respective refractive indices (RI), while the symbol R denotes the radius

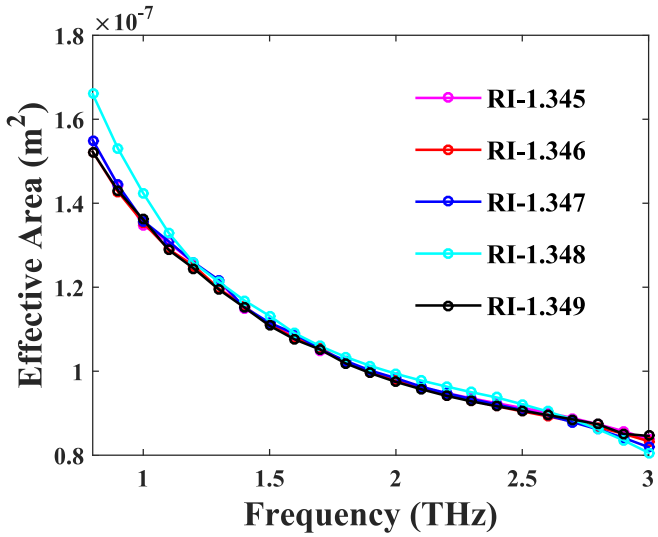

Fig. 7. The frequency-dependent effective area of the model that was presented.

of curvature, r denotes the fiber core radius, and α denotes the fiber's acceptance angle.

For medical imaging, a high NA photonic crystal fiber is preferred. Fig. 8 depicts the suggested sensor's Numerical Aperture (NA). The suggested sensor for the detection of tuberculosis cells has astonishingly minimal confinement loss and high relative sensitivity. Seniority, it is a strong contender for applications involving the detection of tuberculosis due to its mono-mode characteristic. The potential of the sensor in tuberculosis detection is considerable based on the responses for numerical aperture and effective area. This is the first time a tuberculosis sensor based on spectroscopy has been proposed with a sensitivity this high (up to 92 %) and a loss this low. This suggests that the proposed sensor may create new opportunities for the identification and diagnosis of different TB cells.

Due to their susceptibility to leakage, the background materials encountered a diverse range of losses within the core region of the PCF. The primary loss metrics utilized in PCF are confinement loss and EML. In the design of the fiber, ZEONEX is utilized extensively.

By employing the formula [28], the EML can be ascertained:

$$\text{EML}\ (\alpha_{\text{eff}}) = \sqrt{\frac{\varepsilon_0}{\mu_0}} \left(\frac{\int_{\text{mat}} n_{mat}\ |E|^2\ \alpha_{\text{mat}}\ dA}{.5^* \left| \int_{all} (E^* H.z) dA \right|} \right), (\text{cm}^{-1}) \qquad (9)$$

The variables ε_0 and μ_0 denote, respectively, the relative permittivity and permeability of free space. Furthermore, the absorption loss of the material is denoted by α_{mat}, while n_{mat} represents the refractive index (RI) of the material. The expression for the pointing vector equation is $S_z = \frac{1}{2}(E \times H^*)$. H* and E represent the complex parameters of the electric and magnetic fields, respectively.

Pictured in Fig. 9 is the EML. The EML decreases substantially as the frequency increases. 0.0211 cm^{-1} is the EML at an operational frequency of 1 THz. The EML appears to be in a constant mode between 2 and 3 THz. This quantity of EML is inconsequential in relation to the recommended H-PCF.

Fig. 10 shows both polarizations of EMI under optimal design conditions. This study found that the maximum frequency range of 3 THz is represented by the highest peak value of 1.40, which represents the rise of EMI with frequency. At 1 THz, the refractive indices follow EMI principles with values of 1.29, 1.29, 1.30, 1.30, and 1.27 for RI of 1.345, 1.346, 1.347, 1.348, and 1.349 respectively.

In Table 2, the relative sensitivity is shown for the optimum parameters and ± 3 % variations of design parameters (such as air hole size and core diameter) in this structure. Here, we seen that a few variances between the ±3 % variations of relative sensitivity (RS). So, we choose optimum design parameters of relative sensitivity values because it's better optical performance and to detection tuberculosis cell easily.

Finally, Table 3 provides a comparative analysis of the PCF and its optical characteristics as captured by the THz system. The proposed PCFs are subsequently in comparison to the table's standard articles. Other reported PCFs have a lower EML and a greater sensitivity than the H-PCF under consideration, as shown in Table 3.

The intended H-PCF is revealed to have circular air openings only. However, contemporary fabrication techniques such as 3D printing, capillary layering, sol-gel, and drilling hold promise for the production of PCF [39–41]. In addition, it should be noted that the sol-gel and capillary stacking techniques are ideally adapted for the production of circular air holes [42–46]. Hence, it can be inferred that the H-PCF under consideration is easily reproducible using the sol-gel technique. Conversely, the method of selective infill [47] is ideal for loading or filling chemicals (tuberculosis cells for 1.345) into the interior regions of any PCF fiber. We obtained improved guiding properties, with

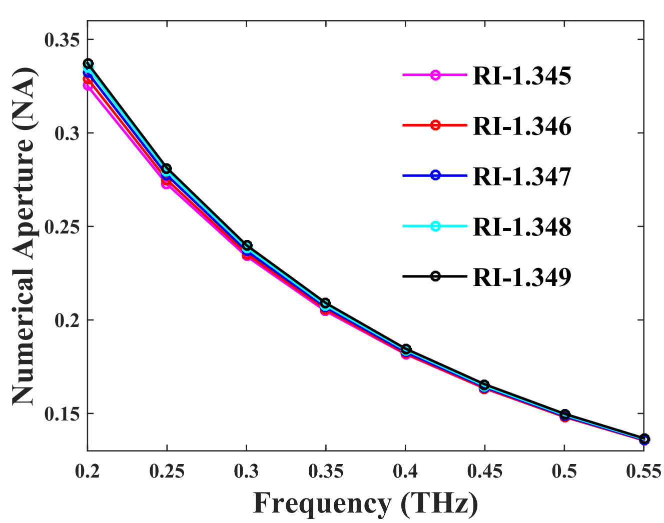

Fig. 8. As demonstrated at different frequencies, the numerical aperture of the model.

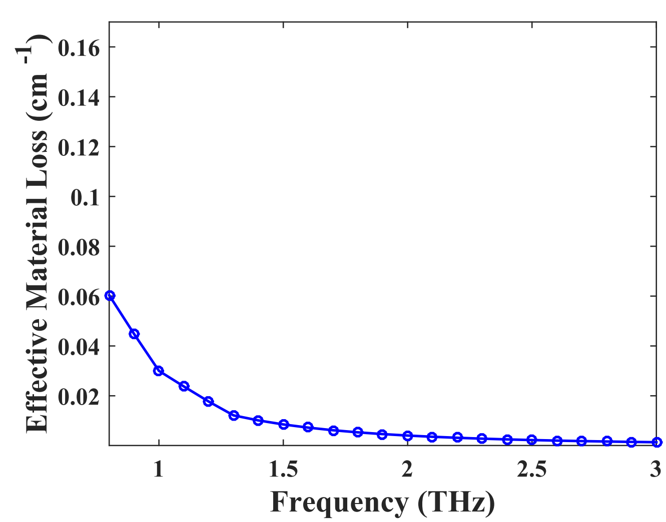

Fig. 9. The recommended PCF for different frequencies results in EML or effective material loss.

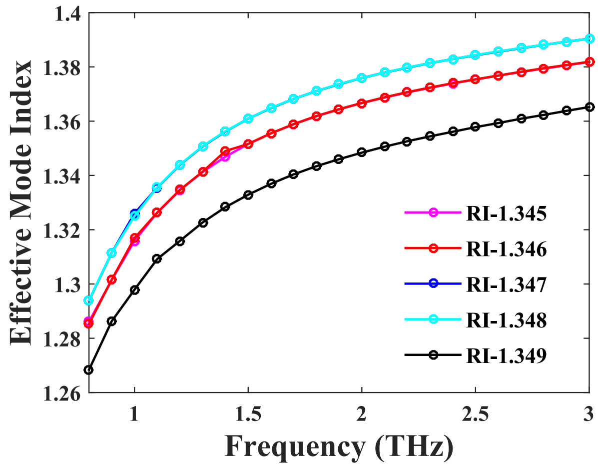

Fig. 10. EMI with respect to the frequencies at the ideal conditions.

Table 2
The relative sensitivity (%) of refractive index (RI) between the optimum parameters and the variations within±3 % at 1 THz.

Parameters (%)	Relative sensitivity (%)of refractive index (RI)				
	1.345	1.346	1.347	1.348	1.349
+ 3 %	91.90 %	89.88 %	91.95 %	91.90 %	87.80 %
Optimum	91.75 %	89.41 %	91.74 %	91.73 %	87.65 %
−3 %	90.20 %,	88.20 %	89.15 %	90.60 %	86.45 %

Table 3
An analysis of the optical characteristics of established PCFs in comparison to the proposed H-PCF.

Ref.	Frequency/ wavelength	Sensed chemical	EML (cm^{-1})	Relative sensitivity (%)
[29]	1.33 μm	Ethanol	–	34.00 %
[30]	1.33 μm	Benzene	–	49.17 %
[31]	1.33 μm	Sulfuric acid	–	63.50 %
[32]	1 THz	Ethanol	0.05	68.87 %
[33]	1.8 THz	HCN	0.031	77.50 %
[34]	1.8 THz	Cyanide	0.023	85.80 %
[35]	1 THz	KCN	0.047	84.52 %
[36]	1.3 THz	KCN	0.005	86.35 %
[37]	1.5 THz	RBCs	–	80.93 %
[38]	1.6 THz	Benzene	–	85.70 %
This Work (H-PCF)	1 THz	tuberculosis cell	0.0211	91.75 %

confinement loss, RS, EA, and EMI included, through the integration of this method of selective filling into a functional research apparatus.

2. Conclusion

An innovative tuberculosis sensor in the form of a hexagon for identifying tuberculosis cells is evaluated based on parameters for example, a V-parameter for the effective area, sensitivity, and confinement loss. Aperture of ZEONEX-based PCF at the operating wavelength of 0.80–3.0 THz. An extremely low loss of 6.30×10^{-8} dB/m is achieved, with a maximal sensitivity of 91.75 % (tuberculosis cell for 1.345). An effective sensor can be identified by the recommended hexagonal PCF's mono-mode behavior throughout the whole operational wavelength range. The suggested sensor is promising for detecting tuberculosis and has better results in Table 3, than the sensors discussed in the preceding section. Here, air holes of different sizes and forms in photonic crystal fibers are examined. Because of its geometric configuration, it is feasible to produce and implement in practical settings. Consequently, this may constitute an innovative methodology for the detection of tuberculosis cell that is notably more precise, economical, and possesses enhanced sensing capabilities in comparison to previous investigations. Consequently, bio-sensing, bio-medical engineering, and other fields relating to sensing will benefit from the structure of H-PCF. These findings validate its potential for effectively detecting these analytics in practical sensing applications.

Ethical approval

No unethical work has been performed in this research work.

Funding

The authors have not received any funding for this research.

CRediT authorship contribution statement

Rakib Hossen: Writing – review & editing, Writing – original draft, Resources, Investigation. **Md. Selim Hossain:** Writing – review & editing, Supervision, Data curation, Conceptualization. **Sadia Afrin Mim:** Data curation, Software, Supervision, Validation. **Md. Al-Amin:** Writing – review & editing, Visualization, Supervision, Conceptualization. **Sabbir Ahmed:** Supervision, Methodology, Formal analysis, Conceptualization. **Md. Ashrafuzzaman:** Formal analysis, Resources, Supervision, Validation. **Md. Ashiq Salahin:** Investigation, Resources, Validation, Visualization. **Shuvo Sen:** Project administration, Formal analysis, Data curation, Conceptualization.

Declaration of competing interest

The Authors declare that they have no conflict of interest.

Data availability

Data sharing is not applicable to this article.

References

[1] T.D. Bradley, Y. Wang, M. Alharbi, B. Debord, C. Fourcade-Dutin, B. Beaudou, F. Gerome, F. Benabid, Optical properties of low loss (70dB/km) hypocycloid-core Kagome hollow core photonic crystal fiber for Rb and Cs based optical applications, J. Lightwave Technol. 31 (16) (2013) 2752–2755.

[2] M. Sharma, N. Borogohain, S. Konar, Index guiding photonic crystal fibers with large birefringence and walk-off, J. Lightwave Technol. 31 (21) (2013) 3339–3344.

[3] Y. Kwon, K. Park, S. Hong, Y. Jeong, Numerical study on the supercontinuum generation in an active highly nonlinear photonic crystal fiber with flattened all-normal dispersion, IEEE J. Quantum Electron. 53 (5) (2017) 1–8.

[4] H. Chen, S. Li, J. Li, Y. Han, Y. Wu, High sensitivity of temperature sensor based on ultracompact photonics crystal fibers, IEEE Photon. J. 6 (6) (2014) 1–6.

[5] N. Ayyanar, D. Vigneswaran, M. Sharma, M. Sumathi, M.M. Rajan, S. Konar, Hydrostatic pressure sensor using high birefringence photonic crystal fibers, IEEE Sensors J. 17 (3) (2016) 650–656.

[6] D. Vigneswaran, N. Ayyanar, M. Sharma, M. Sumathi, M. Rajan, K. Porsezian, Salinity sensor using photonic crystal fiber, Sensors Actuators A Phys. 269 (2018) 22–28.

[7] Sofyan A. Taya, Dana N. Alhamss, Abdulkarem H.M. Almawgani, Ahmad Alzahrani, Ilhami Colak, Shobhit K. Patel, Tuberculosis detection using a low-loss and highly sensitive photonic crystal fiber technique in the terahertz regime, J. Opt. Soc. Am. B 40 (2023) 2382–2391.

[8] J. Qin, B. Zhu, Y. Du, Z. Han, Terahertz detection of toxic gas using a photonic crystal fiber, Opt. Fiber Technol. 52 (2019) 101990.

[9] M.S. Islam, J. Sultana, A. Dinovitser, K. Ahmed, B.W.H. Ng, D. Abbott, Sensing of toxic chemicals using polarized photonic crystal fiber in the terahertz regime, Opt. Commun. 426 (2018) 341–347.

[10] H. Zhang, X. Li, U-fiber-based biosensor for temperature-compensated acetylcholine-specific measurement, Opt. Lett. 48 (2023) 2138–2141.

[11] W. Chen, Z. Li, W. Cheng, T. Wu, Surface plasmon resonance biosensor for exosome detection based on reformative tyramine signal amplification activated by molecular aptamer beacon, J. Nanobiotechnol. 19 (2021) 450.

[12] Y. Huang, Y. Wang, G. Xu, Compact surface Plasmon resonance IgG sensor based on H-shaped optical Fiber, Biosensors 12 (2022) 141.
[13] S.K. Srivastava, C.J. Van Rijn, M.A. Jongsma, Biosensor-based detection of tuberculosis, RSC Adv. 6 (22) (2016) 17759–17771.
[14] M. Trzaskowski, A. Napiórkowska, E. Augustynowicz-Kopeć, T. Ciach, Detection of tuberculosis in patients with the use of portable SPR device, Sensors Actuators B Chem. 260 (2018) 786–792.
[15] G.T. Noordhoek, A.H. Kolk, G. Bjune, D. Catty, J.W. Dale, P.E. Fine, P. Godfrey-Faussett, S.N. Cho, T. Shinnick, S.B. Svenson, Sensitivity and specificity of PCR for detection of Mycobacterium tuberculosis: a blind comparison study among seven laboratories, J. Clin. Microbiol. 32 (2) (1994) 277–284.
[16] K. Arora, S. Chand, B.D. Malhotra, Recent developments in bio-molecular electronics techniques for food pathogens, Anal. Chim. Acta 568 (1–2) (2006) 259–274.
[17] M.A. Jabin, K. Ahmed, M.J. Rana, B.K. Paul, M. Islam, D. Vigneswaran, M.S. Uddin, Surface plasmon resonance based titanium coated biosensor for cancer cell detection, IEEE Photon. J. 11 (4) (2019) 1–10.
[18] M.S. Islam, J. Sultana, K. Ahmed, M.R. Islam, A. Dinovitser, B.W.H. Ng, D. Abbott, A novel approach for spectroscopic chemical identification using photonic crystal fiber in the terahertz regime, IEEE Sensors J. 18 (2) (2017) 575–582.
[19] S.H. Hsu, S.C. Hung, Y.K. Chen, Z.H. Jian, Surface plasmon resonator using high sensitive resonance telecommunication wavelengths for DNA sensors of Mycobacterium tuberculosis with thiol-modified probes, Sensors 15 (1) (2015) 331–340.
[20] Q. Zhang, X. Yang, P. Li, G. Huang, S. Feng, C. Shen, B. Han, X. Zhang, F. Jin, F. Xu, T.J. Lu, Bioinspired engineering of honeycomb structure–using nature to inspire human innovation, Prog. Mater. Sci. 74 (2015) 332–400.
[21] M.M. Hasan, M. Barid, M.S. Hossain, et al., Large effective area with high power fraction in the core region and extremely low effective material loss-based photonic crystal fiber (PCF) in the terahertz (THz) wave pulse for different types of communication sectors, J. Opt. (2021).
[22] S.A. Mitu, D.K. Dey, K. Ahmed, B.K. Paul, Y. Luo, R. Zakaria, V. Dhasarathan, Fe3O4 nanofluid injected photonic crystal fiber for magnetic field sensing applications, J. Magn. Magn. Mater. 494 (2020) 165831.
[23] M.D. Abdullah-Al-Shafi, Nasima Akter, Shuvo Sen, M.D. Selim Hossain, Design and performance analysis of background material of zeonex based high core power fraction and extremely low effective material loss of photonic crystal fiber in the terahertz (THz) wave pulse for many types of communication areas, Optik 243 (2021) 167519. ISSN 0030–4026.
[24] M. De, V.K. Singh, Multi-purpose photonic crystal fiber having advanced optical properties and long sensing range, Photon. and Nanostruct.-Fundament. Applicat. 36 (2019) 100722.
[25] Md. Hossain, Hasan Selim, Md. Mahedi, Shuvo Sen, Md. Mollah, Sarwar Hossain, Mir Mohammad Azad, Simulation and analysis of ultra-low material loss of single-mode photonic crystal fiber in terahertz (THz) spectrum for communication applications, J. Opt. Commun. no (2021).
[26] S. Asaduzzaman, K. Ahmed, T. Bhuiyan, T. Farah, Hybrid photonic crystal fiber in chemical sensing, SpringerPlus 5 (1) (2016) 1–11.
[27] Md. Selim Hossain, Nazmul Hussain, Md. Zakir Hossain, Md. Sakib Zaman, Navid Hasan Rangon, Md. Abdullah-Al-Shafi, Shuvo Sen, Mir Mohammad Azad, Performance analysis of alcohols sensing with optical sensor procedure using circular photonic crystal fiber (C-PCF) in the terahertz regime, Sens. Bio-Sens. Res. 100469 (2021). ISSN 2214-1804.
[28] M.J.B.M. Leon, M.A. Kabir, Design of a liquid sensing photonic crystal fiber with high sensitivity, bireferingence & low confinement loss, Sens. Bio-Sens. Res. 28 (2020) 100335.
[29] H. Ebendorff-Heidepriem, J. Schuppich, A. Dowler, L. Lima-Marques, T.M. Monro, 3D-printed extrusion dies: a versatile approach to optical material processing, Opti. Mater. Express 4 (8) (2014) 1494–1504, https://doi.org/10.1364/OME.4.001494.
[30] R. Islam, M.S. Habib, G.K.M. Hasanuzzaman, S. Rana, M.A. Sadath, C. Markos, IEEE Photon. Technol. Lett. 28 (2016) 1537, https://doi.org/10.1109/lpt.2016.2550205.
[31] M. Nagel, P. Haring Bolivar, M. Brucherseifer, H. Kurz, A. Bosserhoff, R. Büttner, Integrated THz technology for label-free genetic diagnostics, Appl. Phys. Lett. 80 (2002) 154–156, https://doi.org/10.1063/1.1428619.
[32] E. Podder, M.B. Hossain, R.H. Jibon, A.A.M. Bulbul, H.S. Mondal, Chemical sensing through photonic crystal fiber: sulfuric acid detection, Front. Optoelectron. (2019) 1–10.
[33] X. Yang, Y. Lu, B. Liu, J. Yao, Analysis of graphene-based photonic crystal fiber sensor using birefringence and surface plasmon resonance, Plasmonics 12 (2) (2017) 489–496.
[34] M.S. Islam, J. Sultana, A. Dinovitser, K. Ahmed, B.W. Ng, D. Abbott, Sensing of toxic chemicals using polarized photonic crystal fiber in the terahertz regime, Opt. Commun. [Internet]. 426 (2018) 341, https://doi.org/10.1016/j.optcom.2018.05.030.
[35] A.-M. Bulbul, et al., Toxic chemicals detection using photonic crystal Fiber in THz regime, in: In 2020 11th International Conference on Computing, Communication and Networking Technologies (ICCCNT), IEEE, Kharagpur, India, Jul. 2020, pp. 1–5, https://doi.org/10.1109/ICCCNT49239.2020.9225544.
[36] Md.B. Hossain, E. Podder, A.A.-M. Bulbul, H.S. Mondal, M. Raihan, Md.T. Islam, Identification of cyanide within hollow Core photonics crystal Fiber, in: In 2019 10th International Conference on Computing, Communication and Networking Technologies (ICCCNT), IEEE, Kanpur, India, Jul. 2019, pp. 1–4, https://doi.org/10.1109/ICCCNT45670.2019.8944499.
[37] K. Ahmed, et al., Refractive index-based blood components sensing in terahertz Spectrum, IEEE Sensors J. 19 (9) (May 2019) 3368–3375, https://doi.org/10.1109/JSEN.2019.2895166.
[38] M.S. Islam, J. Sultana, K. Ahmed, M.R. Islam, A. Dinovitser, B.W. Ng, et al., A novel approach for spectroscopic chemical identification using photonic crystal fiber in the terahertz regime, IEEE Sensors J. 18 (2018) 575–582, https://doi.org/10.1109/JSEN.2017.2775642.
[39] H.D. Inci, S. Ozsoy, A theoretical study of large solid-core square-lattice silica photonic crystal fibers with square air-holes, Opt. Mater. 35 (2) (2012) 205–210.
[40] R. Islam, M.S. Habib, G.K.M. Hasanuzzaman, S. Rana, M.A. Sadath, C. Markos, A novel low-loss diamond-core porous fiber for polarization maintaining terahertz transmission, IEEE Photon. Technol. Lett. 28 (14) (2016) 1537–1540.
[41] S. Chowdhury, S. Sen, K. Ahmed, S. Asaduzzaman, Design of highly sensible porous shaped photonic crystal fiber with strong confinement field for optical sensing, Optik 142 (2017) 541–549.
[42] D. Pysz, I. Kujawa, R. Stepien, M. Klimczak, A. Filipkowski, M. Franczyk, L. Kociszewski, J. Buzniak, K. Haraśny, R. Buczynski, Stack and draw fabrication of soft glass microstructured fiber optics, Bull. Polish Acad. of Sci.-Techn. Sci. 62 (2014) 667–682.
[43] Abdel Salam Hamdy Makhlouf, Rocio Rodriguez, Chapter 15 - bioinspired smart coatings and engineering materials for industrial and biomedical applications, in: Abdel Salam Hamdy Makhlouf, Nedal Y. Abu-Thabit (Eds.), Advances in Smart Coatings and Thin Films for Future Industrial and Biomedical Engineering Applications, Elsevier, 2020, pp. 407–427.
[44] C.J. Brinker, K.D. KeeferDale, W. SchaeferDale, W. Schaefer, C.S. Ashley, Sol-gel transition in simple silicates, J. Non-Crystalli. Solids 48 (1982) 47.
[45] A.H. Aly, D. Mohamed, Z.A. Zaky, Z.S. Matar, N.S. Abd El-Gawaad, A.S. Shalaby, F. Tayeboun, M. Mohaseb, Novel biosensor detection of tuberculosis based on photonic band gap materials, Mater. Res. 24 (2021).
[46] Rayhan Habib Jibon, et al., Design mechanism and performance evaluation of photonic crystal fiber (PCF)-based sensor in the THz regime for sensing noxious chemical substrates of poultry feed, Appli. Phys. A 128 (2) (2022) 1–9.
[47] A.H.M. Iftekharul Ferdous, et al., A heptagonal PCF-based oil sensor to detect fuel adulteration using terahertz spectrum, Sens. Bio-Sens. Res. 36 (2022) 100485.